Jinx, an MCMV susceptibility phenotype caused by disruption of *Unc13d*: a mouse model of type 3 familial hemophagocytic lymphohistiocytosis

Karine Crozat,[1] Kasper Hoebe,[1] Sophie Ugolini,[2,3,4] Nancy A. Hong,[5] Edith Janssen,[6] Sophie Rutschmann,[1] Suzanne Mudd,[1] Sosathya Sovath,[1] Eric Vivier,[2,3,4] and Bruce Beutler[1]

[1]The Scripps Research Institute (TSRI), La Jolla, CA 92037
[2]Centre d'Immunologie de Marseille-Luminy (CIML), Université de la Méditerranée, Marseille 13288, France
[3]Institut National de la Santé et de la Recherche Médicale (INSERM), U631, Marseille 13288, France
[4]Centre National de la Recherche Scientifique (CNRS), UMR6102, Marseille 13288, France
[5]Phenomix Corporation, San Diego, CA 92121
[6]La Jolla Institute for Allergy and Immunology, La Jolla, CA 92037

Mouse cytomegalovirus (MCMV) susceptibility often results from defects of natural killer (NK) cell function. Here we describe *Jinx*, an *N*-ethyl-*N*-nitrosourea–induced MCMV susceptibility mutation that permits unchecked proliferation of the virus, causing death. In *Jinx* homozygotes, activated NK cells and cytotoxic T lymphocytes (CTLs) fail to degranulate, although they retain the ability to produce cytokines, and cytokine levels are markedly elevated in the blood of infected mutant mice. *Jinx* was mapped to mouse chromosome 11 on a total of 246 meioses and confined to a 4.60–million basepair critical region encompassing 122 annotated genes. The phenotype was ascribed to the creation of a novel donor splice site in *Unc13d*, the mouse orthologue of human MUNC13-4, in which mutations cause type 3 familial hemophagocytic lymphohistiocytosis (FHL3), a fatal disease marked by massive hepatosplenomegaly, anemia, and thrombocytopenia. *Jinx* mice do not spontaneously develop clinical features of hemophagocytic lymphohistiocytosis (HLH), but do so when infected with lymphocytic choriomeningitis virus, exhibiting hyperactivation of CTLs and antigen-presenting cells, and inadequate restriction of viral proliferation. In contrast, neither *Listeria monocytogenes* nor MCMV induces the syndrome. In mice, the HLH phenotype is conditional, which suggests the existence of a specific infectious trigger of FHL3 in humans.

CORRESPONDENCE
Bruce Beutler:
bruce@scripps.edu

Abbreviations used: β2m, β2-microglobulin; C2, Ca^{2+}-binding; ENU, *N*-ethyl-*N*-nitrosourea; FHL3, type 3 familial hemophagocytic lymphohistiocytosis; HLH, hemophagocytic lymphohistiocytosis; LCMV, lymphocytic choriomeningitis virus; Mb, million basepair; MCMV, mouse cytomegalovirus; MHD, MUNC homology domain.

Mouse cytomegalovirus (MCMV) is a β-herpesvirus that is contained by the host through the action of NK cells before the onset of the adaptive immune response. Mice of the C57BL/6 or C57BL/10 background show robust resistance to MCMV due to the expression of the NK cell–activating receptor Ly49H, whereas BALB/c mice, lacking Ly49H, are highly susceptible (1–4).

We have previously described a genetic screen for susceptibility to MCMV, performed in C57BL/6 mice homozygous for random *N*-ethyl-*N*-nitrosourea (ENU)-induced germline mutations (5). Based on the frequency of transmissible susceptibility mutations, we have estimated that ∼300 genes comprise the MCMV resistome: that set of genes with nonredundant function in early resistance to this pathogen (6).

Among the known components of the resistome are genes required to sense virally encoded nucleic acids and proteins (e.g., *Tlr9*, *Tlr3*, *Myd88*, *Trif*, *Unc93b1*, *Ly49h*, and *Dap12* genes; references 1 and 7–12). Also within the resistome are genes coding for several cytokine mediators (13–16), their receptors (13, 15), and their transducers (5, 17–20). In addition, several genes code for components of the cellular machinery required for NK cell granule exocytosis, or components of the granules themselves. These include *Lyst* (21), *Prf1* (22), and

S. Rutschmann's present address is Dept. of Immunology, Faculty of Medicine, Imperial College London SW7 2AZ, London, UK.

The online version of this article contains supplemental material.

The Journal of Experimental Medicine

genes defective in Griscelli syndrome type II (23) or the Hermansky-Pudlak syndrome type II (unpublished data). Notable in this context is the fact that among proteins involved in granule exocytosis, many contribute to melanosome and/or neuronal exocytosis; hence, complex phenotypes are observed in which mutations that affect pigmentation may also have immunological or neurological consequences (24).

As described previously (5), the *Jinx* mutation [MGI: 3626342], one of eight defects identified by screening 3,500 G3 mutant mice for MCMV susceptibility, is associated with exaggerated cytokine production after MCMV inoculation, consistent with the preservation of innate immune sensing function and inadequate effector function. *Jinx* does not cause aberrant pigmentation or obvious neurological dysfunction. Here we report the detailed phenotypic characterization and positional cloning of *Jinx*, which represents the first animal model of type 3 familial hemophagocytic lymphohistiocytosis (FHL3) in humans. We show that in the mouse, the hemophagocytic lymphohistiocytosis (HLH) phenotype is conditional, in that it depends upon a specific infectious trigger.

RESULTS

The *Jinx* phenotype

When inoculated with 10^5 PFU of Smith strain MCMV, WT C57BL/6 mice normally survive infection, showing no sign of illness, and when killed after 5 d, show very few PFU in the spleen. The *Jinx* mutation was detected in a G3 mouse that showed severe illness after inoculation with 10^5 PFU of MCMV. It was retrieved by recrossing the corresponding G1 sire and G2 dam, and then brought to homozygosity by repeated sibling inbreeding. All *Jinx* mice were normally pigmented and showed normal cage activities, and their primary and secondary lymphoid organs were grossly normal in appearance. No abnormalities of lymphoid subsets were evident on CD4, CD8, B220, and NK1.1 typing, nor was there evidence of anemia or a bleeding diathesis (not depicted).

5 d after MCMV infection, viral titers in BALB/c mice and *Jinx* homozygotes are four to five orders of magnitude higher than in WT C57BL/6 mice (Fig. 1 A). Although *Jinx* homozygotes do not usually die after challenge with 10^5 PFU of MCMV, an inoculum of 2.5×10^5 PFU is uniformly lethal to both *Jinx* and BALB/c mice within the same time frame (Fig. 1 B). *Jinx* homozygotes show exaggerated production of IL-12, IFN-γ, and IFN-α/β (type I IFN) 36 h after inoculation with the virus (Fig. 1 C). This finding is consistent with normal sensing by APCs in the context of an inadequate NK cell effector response, permitting unfettered accumulation of the virus and therefore a stronger stimulus for cytokine production.

Because NK cells are pivotal in resistance to acute infection with MCMV, we sought to analyze NK cytolytic activity and IFN-γ production because defects in either of these processes would suggest an explanation for the observed failure to restrict viral proliferation within infected tissues. In *Jinx* mutants, NK cell–mediated cytotoxicity against β2-microglobulin (β2m)-deficient target cells in vivo (Fig. 2 A) and against YAC-1 cells in vitro (Fig. 2 B) is abolished. However, NK cells from MCMV-infected *Jinx* mice are able to be activated as indicated by their ability to secrete normal levels of IFN-γ (Fig. 2 C). Accordingly, we suspected a problem with NK cell degranulation and used the CD107a surface translocation method (25, 26) to assess degranulation in *Jinx* and WT NK cells. A gross abnormality of NK cell granule exocytosis was

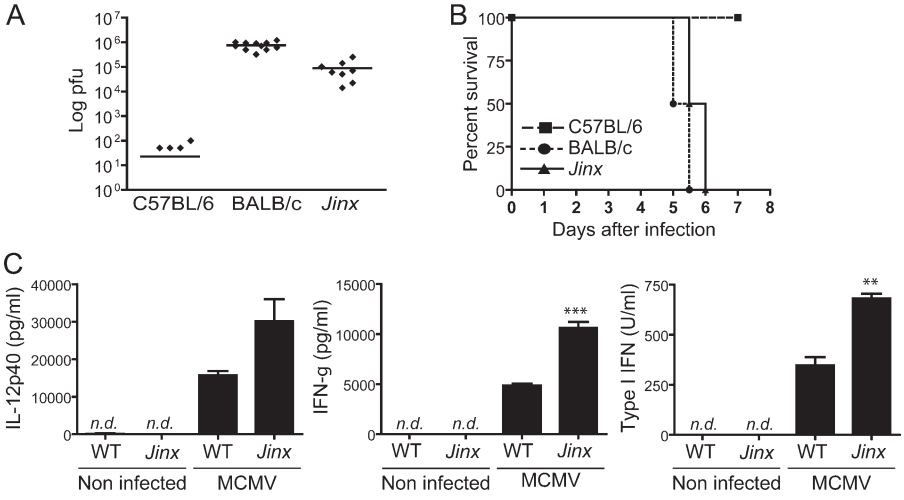

Figure 1. *Jinx* mutants show high susceptibility and an increase in cytokine production after MCMV infection. (A) PFU were measured in spleens from C57BL/6, BALB/c, and *Jinx/Jinx* mice on day 5 after the inoculation with 10^5 PFU of MCMV. BALB/c mice were used as controls for susceptibility. Each point represents an individual animal, and lines refer to means. (B) Time-dependent death of C57BL/6 mice, BALB/c mice, and *Jinx/Jinx* mutants when challenged with 2.5×10^5 PFU of MCMV. For each genotype, $n = 6$. The experiment was concluded after 7 d, but no additional deaths were observed for at least 10 additional days. (C) IL-12p40, IFN-γ, and IFN-α/β levels in serum measured 36 h after MCMV infection. *n.d.*, not detected.

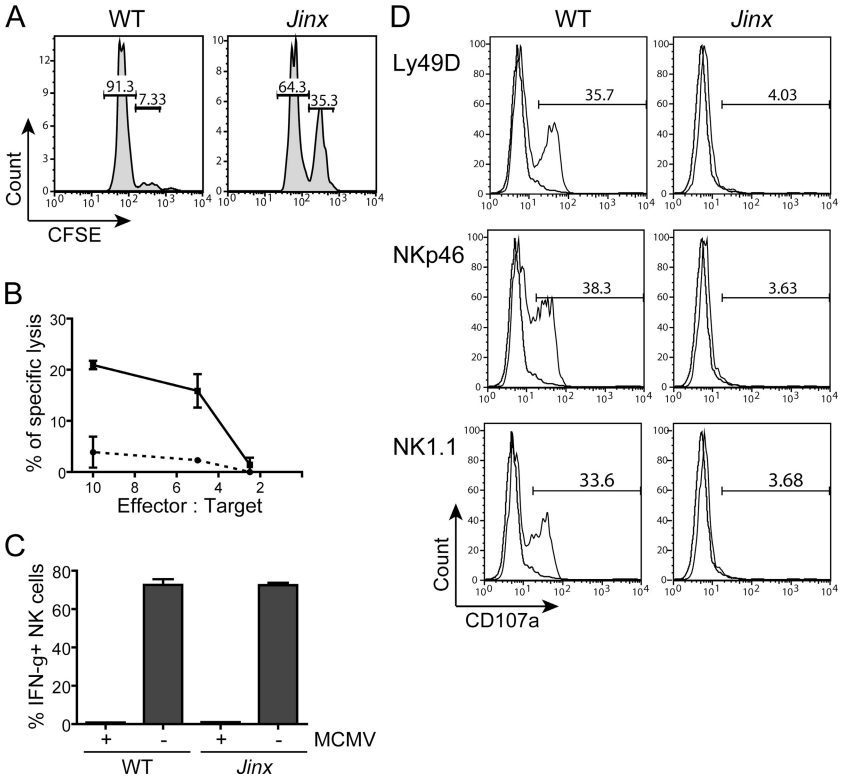

Figure 2. *Jinx* NK cells produce IFN-γ after MCMV infection but fail to kill target cells due to a defect in degranulation. (A) In vivo assay of NK cell killing. WT, cells were injected into C57BL/6 mouse; *Jinx*, cells injected into a *Jinx/Jinx* homozygote. Numbers refer to the percentage of cells in each gate. (B) Killing of YAC-1 cells in vitro by NK cells purified from MCMV-infected *Jinx* homozygotes (dashed line) or C57BL/6 cells (solid line). (C) IFN-γ production by NK cells obtained from MCMV-infected C57BL/6 (WT) and *Jinx/Jinx* homozygotes 2 d after inoculation. Data show the percentage of IFN-γ^+ cells among the gated NK1.1$^+$ CD3ε^- population. (D) Stimulus-induced degranulation of NK cells measured by CD107a surface expression. Plate-bound antibodies specific for some NK cell receptors (solid line) or their respective isotype controls (faded line) were used for induction. Numbers indicate the percentage of NK1.1$^+$ CD3ε^- cells expressing CD107a at their surface.

observed, as reflected by the failure to transfer CD107a to the cell surface in response to stimulation by NK cell–activating receptors Ly49D, NKp46, or NK1.1 (Fig. 2 D).

When we examined CTL function in *Jinx* homozygotes, a similar phenotype was evident. Polyclonal stimulation of CTLs from *Jinx* homozygotes revealed a profound defect in their ability to degranulate (Fig. 3 A), but normal production of IFN-γ was apparent (Fig. 3 B). We therefore inferred that the *Jinx* defect likely involved a component of machinery for exocytosis and, further, concluded that the protein in question had nonredundant function in lymphoid cells but was not required for an analogous function in melanocytes or neurons because melanosome exocytosis to the hair shaft and neurological function was at least grossly intact. Moreover, *Jinx* homozygotes showed no obvious enhancement of susceptibility to *Listeria monocytogenes* (not depicted), consistent with the conclusion that the protein affected has no essential role in neutrophil function.

Positional cloning of *Jinx*

The *Jinx* mutation was mapped by outcrossing the mutant stock to mice of the C57BL/10 and C3H/HeN strains and

Table I. Markers used for *Jinx* fine mapping

Markers	Position (Mb)	Susceptible	Susceptible	Resistant	Resistant
c11.110.56	110.56	D	S-B	S-B	S-B
d11mit291	112.59	D	S-B	S-B	S-B
c11.113.1	113.03	S-B	S-B	S-B	D
c11.115.2	115.46	S-B	S-B	D	D
d11mit203	116.18	S-B	S-B	D	D
c11.117.1	117.63	S-B	D	D	D

The marker positions are derived from Ensembl build 41 database. S-B, single-B6 (homozygous B6 allele); D, double (heterozygous B6-C3H allele).

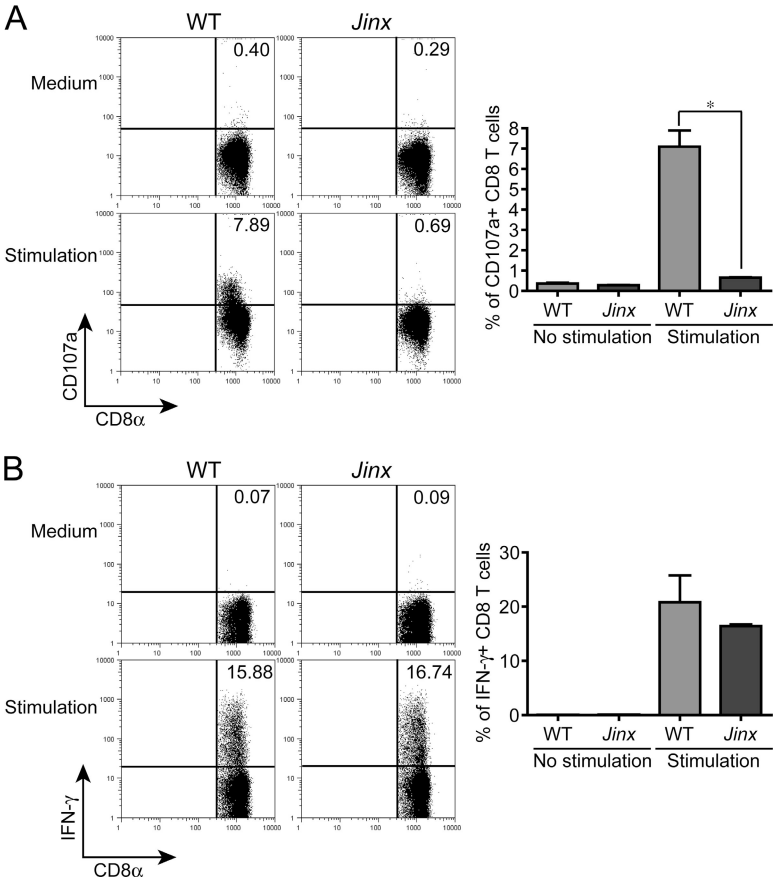

Figure 3. *Jinx* CD8$^+$ T cells produce a normal amount of IFN-γ upon polyclonal stimulation with PMA/ionomycin but fail to degranulate. (A) Surface expression of CD107a. Inset numbers indicate percentage of cells with induced expression. (B) Up-regulation of intracellular IFN-γ. Graphs beneath each FACS illustration show data for three mice.

backcrossing F1 animals to mice of the mutant stock. Using a panel of 68 informative single nucleotide polymorphisms and microsatellite markers to examine 30 meioses derived from the C57BL/10 cross and phenotyping based on MCMV susceptibility, the mutation was mapped to the distal end of chromosome 11 with a log odds distance score of 5.5 (Fig. 4 A). On 216 additional meioses derived from the C3H/HeN cross and phenotyping based on MCMV susceptibility, the mutation was confined to a region circumscribed by markers at 113.03 million basepairs (Mb) and 117.63 Mb removed from the centromere (Ensembl Build 41; Table I). This 4.60-Mb region encompassed 122 annotated genes, 22 of which were excluded from consideration by DNA sequencing, most of them at the cDNA level (Table II).

The *Unc13d* gene was considered as a candidate because mutations in the human orthologue MUNC13-4 cause FHL3, a disease in which CTL and NK cells from affected patients show a defect of degranulation (27, 28). When the *Unc13d* cDNA was amplified from splenocyte mRNA derived from *Jinx* mice and sequence, a 53-bp insertion (degeneration to double sequence) was observed (GenBank accession no. EF127645) in a portion of the cDNA corresponding to exon 26 of the gene.

Further sequencing at the genomic level disclosed a G→T transversion at position 4,538 downstream from the distal end of exon 26 (Fig. 4 B), which created a new donor splice site, preferred to the complete exclusion of the normal donor site (Fig. 4 C). As confirmed by genomic sequencing (GenBank accession no. EF127646), this splicing defect causes the aberrant incorporation of the 53 intronic nucleotides that normally follow exon 26 into the *Unc13d*^{Jinx}-derived mRNA, which in turn leads to the incorporation of 20 aberrant amino acids into the UNC-13D protein, followed by premature termination of the polypeptide chain due to an in-frame TGA codon after amino acid 859 (Fig. 4 D). Normally, 1,085 amino acids in length, the UNC-13D protein features two Ca^{2+}-binding (C2) domains separated by two "MUNC homology" domains (MHDs) and a domain of unknown function (DUF1041; Fig. 4 D). The *Jinx* mutation is predicted to eliminate the second of the C2 domains and part of the second MHD. C2 domains are also found in phospholipases, protein kinases C, and in other members of the MHD-defined family, and extend across many eukaryotic species, including *Caenorhabditis elegans* and *Drosophila melanogaster*. C2 domains appear to bind phospholipids, inositol polyphosphates,

and intracellular proteins, consistent with a possible role in signal transduction.

Conditional induction of an FHL3-like phenotype by lymphocytic choriomeningitis virus (LCMV) infection

FHL3 is a severe disease that occurs in children with mutations of MUNC13-4, the human orthologue of *Unc13d* (27). Although the pathogenesis of the disease is not well understood, the clinical features of the disorder include massive hepatosplenomegaly, thrombocytopenia, neutropenia, and anemia. The two principal hallmarks of the disease are an overwhelming proliferation of $CD8^+$ T cells and macrophages, associated with sustained production of cytokines. Histologically, macrophages are seen to ingest erythroid precursors as well as erythrocytes and platelets. Other forms of FHL occur as a result of mutations in the perforin-encoding gene (29) and the syntaxin-11 gene (30). Some (but not all) features of FHL can be observed in patients with Griscelli syndrome type II (caused by mutations of *RAB27A*; reference 31) and in patients with Chediak-Higashi syndrome (caused by mutations in *LYST*; reference 32).

It has been proposed that an infectious trigger—either viruses such as EBV or intracellular bacteria (33)—is required for expression of the FHL phenotype, a possibility supported by the observation that in *Prf1* mutant mice, *L. monocytogenes* causes increased $CD8^+$ T cell activation (34) and LCMV

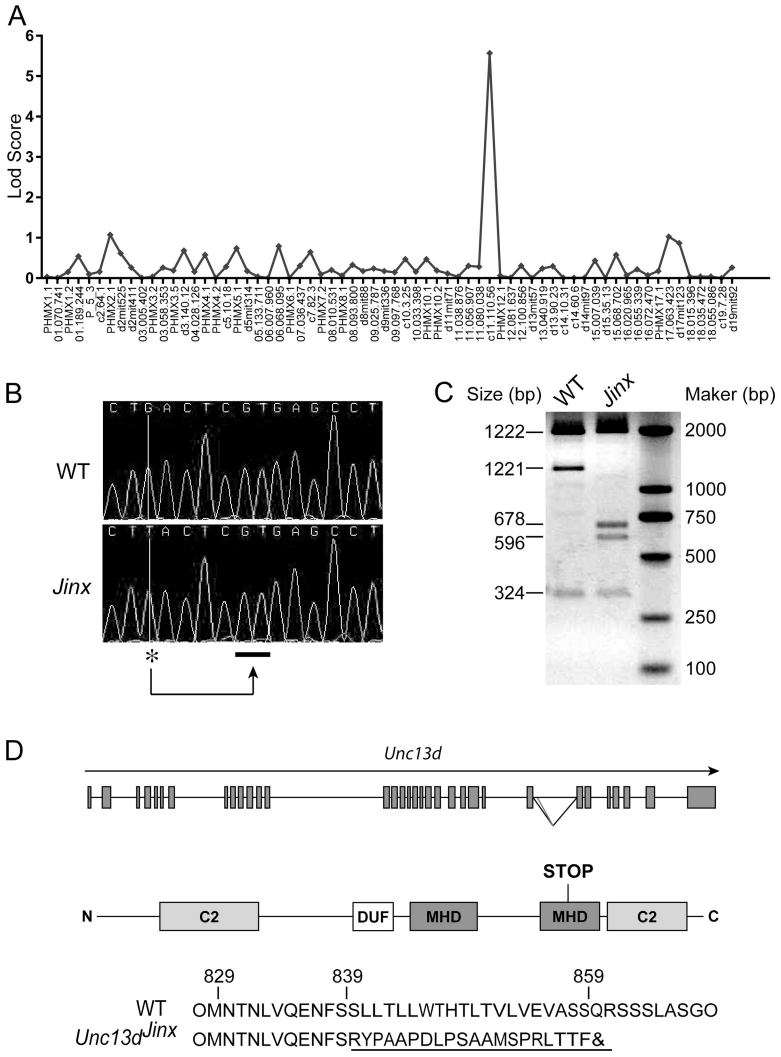

Figure 4. Mapping and positional cloning of *Jinx* (A) Genome-wide confinement of the phenotype on 30 meioses using a panel of 68 informative markers (bottom). Strongest linkage observed with a marker on chromosome 11, 110.56 Mb. (B) Genomic sequence from a part of intron 26 of *Unc13d* reveals a G→T transversion (*), which causes splicing to occur distally (underscore), causing incorporation of 53 bp of intronic sequence into exon 26. (C) Effect of the *Jinx* mutation at the mRNA level. KpnI cuts the WT cDNA twice with a 3,467-bp amplification fragment leading to 1,922-, 1,221-, and 324-bp bands. In *Jinx*, the 53-bp insertion contains an additional KpnI site, giving 1,922-, 596-, 678-, and 324-bp bands. In the mutant cDNA pool, no WT transcript is detectable. (D) Location of *Jinx* mutation in the genomic sequence of *Unc13d* and the structure of the truncated protein predicted from the *Jinx* mutation. C2, Ca^{2+}-binding domain; MHD, MUNC homology domain; DUF, DUF1041 domain.

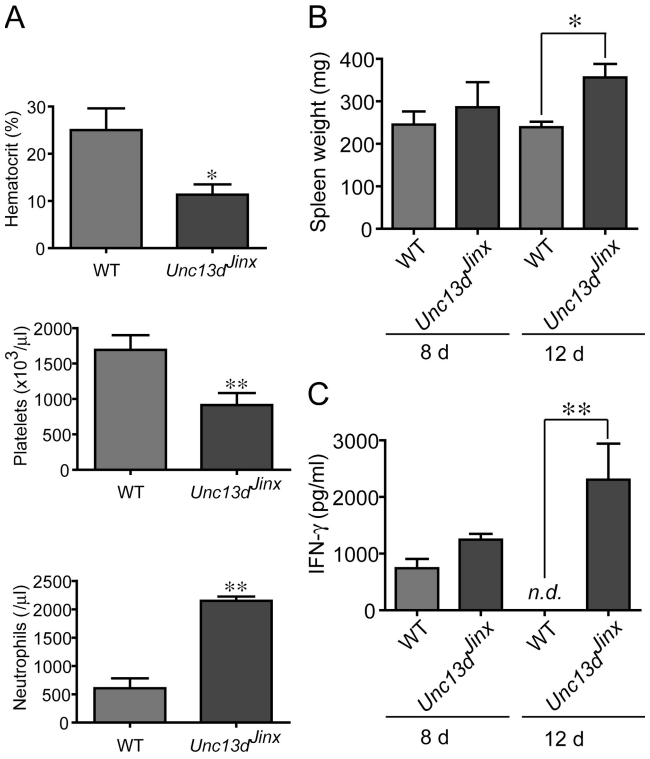

Figure 5. *Unc13d*$^{Jinx/Jinx}$ mice develop an FHL-like phenotype when infected with LCMV. (A) Hematocrit, platelet count, and neutrophil count in the blood of LCMV-infected WT and *Unc13d*$^{Jinx/Jinx}$ mice 12 d after infection. (B) IFN-γ production in the serum of LCMV-infected WT and *Unc13d*$^{Jinx/Jinx}$ mice 8 and 12 d after infection. *n.d.*, not detected. (C) Spleen weight in WT and *Unc13d*$^{Jinx/Jinx}$ mice 12 d after infection. $n = 3$ mice per group.

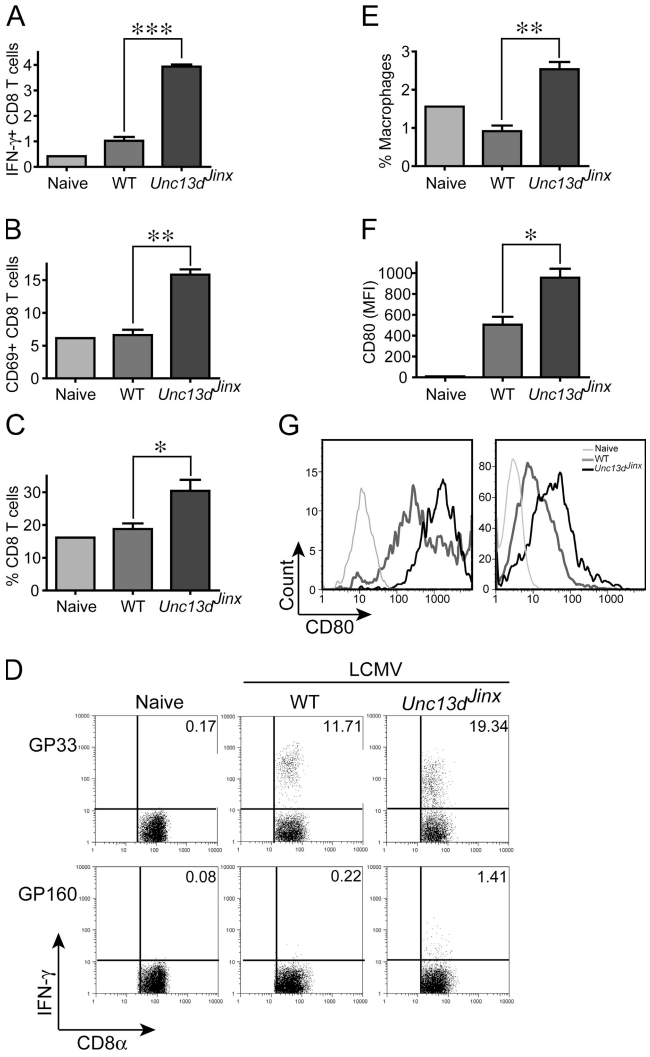

Figure 6. Phenotype of CD8$^+$ T cells and APCs in *Unc13d*$^{Jinx/Jinx}$ mutants after LCMV infection. (A–D) Splenocytes from *Unc13d*$^{Jinx/Jinx}$ or WT mice infected with LCMV 12 d previously or uninfected controls were stained for CD8α, CD3ε, CD69, and IFN-γ. (A) The percentage of IFN-γ$^+$ CD8$^+$ T cells. (B) Percentage of CD69$^+$ CD8α$^+$ T cells. (C) The percentage of CD8α$^+$ CD3ε$^+$ T cells among all splenocytes. (D) Splenocytes were stimulated for 4 h in the presence of LCMV-specific peptide GP33 or the irrelevant peptide GP160. Inset numbers represent the percentage of CD8α$^+$ CD3ε$^+$ IFN-γ$^+$ cells. (E) The percentage of macrophages (F4/80$^+$ CD11b$^+$ cells) among all splenocytes. (F) The expression of CD80 (mean fluorescence intensity) by splenic macrophages (gated on the F4/80$^+$ and CD11b$^+$ population). (G) CD80 up-regulation in macrophages (left) and dendritic cells (right) in uninfected mice and in infected WT and *Unc13d*$^{Jinx/Jinx}$ mice. A single uninfected (naive) mouse was used in all experiments, and a representative set of individual mice were used in D and G. For all other panels, $n = 3$.

infection causes both uncontrolled CD8$^+$ T cell expansion and hepatosplenomegaly (35–37). In *Unc13d*$^{Jinx/Jinx}$ mice, hepatosplenomegaly is neither observed in uninfected animals maintained under standard conditions of housing nor in animals deliberately infected with *L. monocytogenes*, sustaining 7 d of documented infection and followed through 2 wk, whereon all mice recovered (not depicted). Moreover, when 2×10^4 PFU of MCMV are administered to *Unc13d*$^{Jinx/Jinx}$ mice, sickness develops by day 5, but through 12 d of observation, when sickness has fully resolved, there is no evidence of HLH. At day 7, there is neutrophilia (fourfold higher than in WT mice) and monocytosis (threefold higher than in WT mice). The neutrophilia resolves by day 14, whereas the monocytosis does not (Fig. S1, available at http://www.jem.org/cgi/content/full/jem.20062447/DC1). The liver, spleen, and salivary glands all remain normal in size and appearance.

However, HLH can be induced by at least one infectious agent. When infected with LCMV (Armstrong strain) and examined after 12 d, mice have severe anemia and very significant thrombocytopenia, but neutrophilia rather than neutropenia (Fig. 5 A). Splenomegaly (Fig. 5 B) and sustained elevation of IFN-γ in serum (Fig. 5 C) were also present, both hallmarks of the human disease process. Exaggerated production of IFN-γ is evident in splenic CD8$^+$ T cells from infected *Unc13d*$^{Jinx/Jinx}$ mice (Fig. 6 A) as is the activation marker CD69 (Fig. 6 B). The percentage of CD8$^+$ T cells is approximately doubled in the spleen (Fig. 6 C). Similarly doubled with respect to the response observed in WT control

Table II. List and positions of the sequenced genes localized in the *Jinx* critical region

Start position (Mb)	Ensembl gene ID	Description	Level sequenced
113.55	ENSMUSG00000041598	CDC42 effector protein 4	cDNA
114.71	ENSMUSG00000034652	CD300A antigen	cDNA and Genomic
114.75	ENSMUSG00000063193	CD300 antigen like family member B	cDNA and Genomic
114.78	ENSMUSG00000058728	CD300C antigen	cDNA and Genomic
114.80	ENSMUSG00000034641	RIKEN cDNA 4732429D16	Genomic
114.82	ENSMUSG00000044811	CD300A antigen	cDNA and Genomic
114.83	ENSMUSG00000069610		cDNA and Genomic
114.84	ENSMUSG00000069609		cDNA and Genomic
114.85	ENSMUSG00000069608		cDNA and Genomic
114.86	ENSMUSG00000069607	CMRF-35-like molecule 3	cDNA and Genomic
114.87	ENSMUSG00000048498	CD300 antigen like family member E	cDNA and Genomic
114.91	ENSMUSG00000020732	RAB37, member of RAS oncogene	cDNA
114.94	ENSMUSG00000047798	CD300 antigen like family member F	cDNA and Genomic
115.41	ENSMUSG00000020740	ARF binding protein 3	cDNA
115.46	ENSMUSG00000059923	growth factor receptor bound protein 2	cDNA
115.75	ENSMUSG00000020755	transcriptional regulator protein	cDNA
115.90	**ENSMUSG00000057948**	**unc-13 homolog D (C. elegans)**	**cDNA and Genomic**
115.96	ENSMUSG00000020776	Fas (TNFRSF6) binding factor 1	cDNA
116.11	ENSMUSG00000020792	exocyst complex component 7	cDNA
116.15	ENSMUSG00000034227	forkhead box J1	cDNA
116.93	ENSMUSG00000061878	Sphingosine kinase 1	cDNA
116.93	ENSMUSG00000020823	Sec14-like 1	cDNA

Out of 22 sequenced genes, *Unc13d* was the only gene to be mutated (bold type). All positions and descriptions are derived from the Ensembl Build 41 database (www.ensembl.org).

mice are the number of $Unc13d^{Jinx/Jinx}$ splenic $CD8^+$ T cells that respond to GP33 peptide, derived from LCMV (Fig. 6 D). In $Unc13d^{Jinx/Jinx}$ mice, an approximately 2.5-fold increase in the number of $F4/80^+/CD11b^+$ cells were present in the spleen (Fig. 6 E). Among the cells of this population, the APC activation marker CD80 is abnormally up-regulated in $Unc13d^{Jinx/Jinx}$ mice (Fig. 6 F). This up-regulation applied equally in both macrophage and DC populations (Figs. 6 H).

Despite evidence of exaggerated innate and adaptive immune responses to infection, $Unc13d^{Jinx/Jinx}$ mice were not able to eradicate the LCMV infection, which grew out of control so that plaque assays of spleen homogenates showed viral titers >1,000-fold higher in $Unc13d^{Jinx/Jinx}$ mice than in WT mice at 12 d after inoculation. Interestingly, some containment was achieved in the liver, where titers declined between days 8 and 12 after inoculation (Fig. 7, A and B).

Histologically at day 12, $Unc13d^{Jinx/Jinx}$ mice showed abundant hepatic granulomata compared with WT mice (Fig. 8 A), and depletion of germinal centers with replacement by macrophages in peripheral lymph nodes (Fig. 8 B). In the bone marrow as well, macrophage infiltration was evident in $Unc13d^{Jinx/Jinx}$ mice (Fig. 8 C), and at high magnification, hemophagocytosis could clearly be observed (Fig. 8 D).

DISCUSSION

In this paper we have reported the first phenovariant allele of *Unc13d* in mice, detected because it caused severe immunocompromise in the setting of MCMV infection. Although mutations of the human orthologue MUNC13-4 have been identified as the cause of FHL3, no animal model of this disorder has previously been identified, and hence, there has been little chance for insight into the environmental "trigger" of this disease, if such exists.

EBV, a γ-herpesvirus, has been suggested to trigger FHL (33), but assignment of cause and effect has been elusive because EBV infection is relatively common and because data on the penetrance of this relatively rare human disorder have not been available. We attempted to induce FHL-like disease in $Unc13d^{Jinx/Jinx}$ mice using the β-herpesvirus MCMV. The acute lethal effect of MCMV infection in $Unc13d^{Jinx/Jinx}$ mice made the experiment impossible to perform with the highest doses normally tolerated by C57BL/6J controls. However, we note that low doses of the virus, sufficient to produce visible sickness in $Unc13d^{Jinx/Jinx}$ mice, were ultimately cleared without producing an HLH-like disease.

LCMV was investigated as an alternative pathogen because NK cells do not play a prominent role in early host defense against this agent. The LCMV-driven HLH phenotype of $Unc13d^{Jinx/Jinx}$ mice is consistent with a model in which the infection is not effectively cleared in the absence of effective CTL degranulation. Viral infection then drives the expansion of APCs (which are themselves actively infected) and $CD8^+$ T cells, which may be infected as well, and which respond to the ongoing antigenic stimulus that the APCs present. We consider that like the arenavirus LCMV, herpesviruses and possibly many other agents might ultimately initiate a comparable

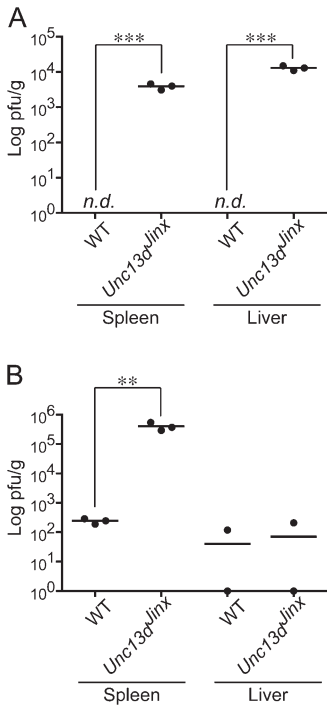

Figure 7. LCMV titre in the liver and spleen after infection in WT and *Unc13d*$^{Jinx/Jinx}$ mice. Standard plaque assays were performed on spleens and livers 8 (A) and 12 d (B) after LCMV infection. *n.d.*, not detected. $n = 3$ mice for each group.

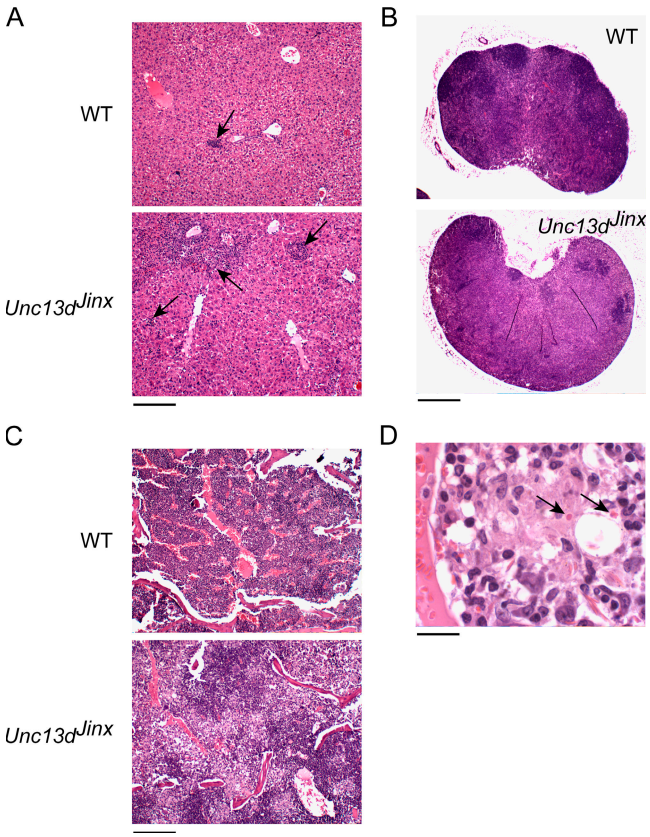

Figure 8. Histologic appearance of the liver and spleen in LCMV-infected *Unc13d*$^{Jinx/Jinx}$ and WT mice displays features of FHL in different organs. Hematoxylin and eosin staining of sections of livers from LCMV-infected *Unc13d*$^{Jinx/Jinx}$ mice (A) showed an increased number of granulomas of larger size (arrow) compared with livers from infected controls (bar, 200 μm). (B) Infiltration of macrophages is observed in lymph nodes in *Unc13d*$^{Jinx/Jinx}$ mice (arrow), along with a paucity of germinal centers (bar, 0.4 mm). (C) Bone marrow from LCMV-infected *Unc13d*$^{Jinx/Jinx}$ mice is heavily infiltrated by macrophages compared with LCMV-infected WT marrow (bar, 200 μm), and at high magnification (D) RBCs are seen to reside within vesicles in bone marrow macrophages (arrows, hemophagocytosis). Bar, 20 μm.

cycle of APC and CTL proliferation that is clinically interpreted as FHL. However, not all microbes will readily cause FHL, and in our initial studies of *Unc13d*$^{Jinx/Jinx}$ mice, *L. monocytogenes* infection was found to be incapable of doing so.

It is interesting to note that the *Unc13d*$^{Jinx/Jinx}$ mice infected with LCMV present one important discrepancy from humans with FHL3: the former show fourfold elevation in peripheral neutrophil counts, whereas FHL3 patients are neutropenic (27, 33, 38, 39). This discrepancy may reflect a different role of the UNC-13D protein in neutrophils in mice as compared with humans, or may alternatively be a property of the microbial inducer that is most commonly culpable in humans. Of interest in this regard, *Prf*$^{-/-}$ mice do develop neutropenia when infected with LCMV (37).

Host resistance mechanisms often incorporate proteins that are multifunctional, not only in the sense that they confer resistance to multiple infectious agents, but also in the sense that they are required for diverse biological processes. Many of the proteins required for NK cell or neutrophil granule exocytosis are also required for pigmentation or have neurological functions. UNC-13D, the protein affected by the *Jinx* mutation, appears to be dedicated to resistance and does not noticeably affect pigmentation or neurological function. Essential in NK cells and CTLs, it is probably dispensable for neutrophil function because defects of neutrophil function usually cause severe immunocompromise during *L. monocytogenes* infection.

UNC-13D is required for priming (fusion competence) of cytoplasmic vesicles. Although we cannot formally exclude the possibility that some functions of UNC-13D might be intact in *Unc13d*$^{Jinx/Jinx}$ homozygotes, it appears most likely that *Unc13d*$^{Jinx/Jinx}$ encodes a completely nonfunctional protein based on deletion/complementation studies of the UNC-13 homologue in *C. elegans*, which have shown that deletion or point mutation within the second MHD abolishes fusion competence and complementation of the motility phenotype (40).

The molecular ancestry of UNC-13D has been traced by homology searches focused on individual domains, such as the C2 domain (41), which is widely distributed in cellular proteins involved in signal transduction or membrane trafficking, and serves as a Ca^{2+}-dependent membrane-targeting module, enabling proteins to bind phospholipids within various

biological membranes. Different C2 domains exhibit lipid selectivity, favoring phosphatidylserine or phosphatidylcholine binding, and the C2 domain of UNC13 from *C. elegans* can engage phorbol esters (42). The DUF1041 motif is often found in conjunction with C2 domains and is represented in several proteins in addition to members of the UNC-13 family, including the brain-specific angiogenesis inhibitor-1–associated protein 3 and the calcium-dependent secretion activator-1 and -2 proteins. The MHD is the signature domain of the MUNC family of proteins and is regarded as an interaction motif based on studies in *C. elegans*, in which it was shown that a double amino acid substitution within the MHD could abolish interaction between UNC-13 and syntaxin (40).

MUNC13-1, MUNC13-2, and MUNC13-3, the closest relatives of MUNC13-4 (UNC13D), are expressed in the brain, and single knockout mutations each produce a CNS phenotype (43–45). Although MUNC13-1 knockouts are often born dead and show relatively severe neurological impairment (43), individual MUNC13-2 and MUNC13-3 mice, and MUNC13-2 and MUNC13-3 double knockouts, are viable (46), consistent with the conclusion that these paralogues serve at least partially redundant functions. Deletion of the more distantly related MUNC18-1–encoding gene *Stxbp1* (syntaxin binding protein-1) causes perinatal lethality related to neurological dysfunction as well (47).

MUNC13-4 (and by implication, UNC-13D) is believed to associate with RAB27A on the basis of immunoprecipitation studies performed with human platelets (48), and is believed to be required for the priming of platelet-dense granules. However, we are unable to find evidence of platelet dysfunction in *Unc13d*$^{Jinx/Jinx}$ homozygotes, suggesting that alternative mechanisms for dense granule priming, independent of UNC-13D, must exist in mice. The strong NK cell phenotype suggests nonredundancy of function, and although it may not apply to all classes of NK cell granules, it is clear that the LAMP1 (CD107a) compartment is forbidden exocytosis in *Unc13d*$^{Jinx/Jinx}$ homozygotes. Fas ligand, granzymes, and perforin colocalize within the same class of vesicles in NK cells (49, 50), and it is therefore likely that in *Unc13d*$^{Jinx/Jinx}$ mice, a defect of Fas ligand release also exists. This may contribute to the proliferative syndrome that is observed, to the extent that Fas ligand initiates apoptosis in the target cell population. However, the absence of spontaneous lymphoproliferative disease in *Unc13d*$^{Jinx/Jinx}$ mice (as compared with *Gld* mice, for example) indicates that the NK cells and CTLs do not act as the essential source of Fas ligand required for homeostatic control of T cells in vivo.

MATERIALS AND METHODS

Mice, ENU mutagenesis, MCMV susceptibility screen, and Jinx mapping. C57BL/6 (also referred to as WT), C57BL/10, C3H/HeN, BALB/c, *β2m*$^{-/-}$, and *Jinx/Jinx* mice (MMRRC:016137) were maintained under specific pathogen-free conditions in the TSRI vivarium, and all studies involving mice were performed in accordance with institutional regulations governing animal care and use. ENU mutagenesis was performed as described previously (51) in a C57BL/6 background, naturally resistant to MCMV infection. Because most inbred strains show either a strong or moderate susceptibility to MCMV infection, the chromosome location of *Jinx* mutation was obtained by outcrossing *Jinx* homozygotes to C57BL/10 mice, and then backcrossing to *Jinx* stock and infecting F2 mice with MCMV at 6 wk of age. For mapping against the C57BL/10 background, 31 informative single nucleotide polymorphisms and 37 microsatellite polymorphisms were used (Table S1, available at http://www.jem.org/cgi/content/full/jem.20062447/DC1), distributed across the genome at ∼50-Mb intervals. For fine mapping, C57BL/10 and C3H/HeN strains were used using the microsatellite markers shown in Table I. Four informative markers were identified in our laboratory and are defined in Table S2).

Viruses, in vivo susceptibility screen, PFU assay, and serum cytokine detection. The generation of the MCMV Smith strain stock from the salivary glands of 3-wk-old MCMV-infected BALB/c mice, as well as the conditions of the in vivo MCMV susceptibility screen of ENU germline mutants, was described previously (5). MCMV was administrated i.p. The Armstrong strain of LCMV (provided by E. Zuniga and M.B.A. Oldstone, TSRI, La Jolla, CA) was injected i.p. at 10^5 PFU per mouse. Viral loads were determined after organ homogenization in DMEM, 3% FCS, by standard plaque assays on 3T3-NIH cells for MCMV (52) and on VERO cells for LCMV (53).

Serum cytokine detection and complete blood counts. 36 h after MCMV infection or at the times indicated after LCMV infection, mice were bled from the retroorbital sinus, and the concentration of IL-12p40, TNF-α, IL-6, and IFN-γ in the serum was assayed by ELISA (eBioscience). The bioactivity of serum type I IFN was measured by luciferase assay using L929-ISRE cells as described previously (5). Complete blood cells counts were performed by Antech Diagnostics.

In vivo assay for NK cell cytotoxic activity. Splenic suspensions from β2m-deficient mice and C57BL/6 controls were resuspended at 10^7 cells/ml in PBS. Control and target splenocytes were, respectively, labeled with a low and high concentration of CFSE at room temperature for 10 min. The labeling was stopped by dumping cold FCS on cell suspensions. Cells were washed twice, counted, and resuspended at 5×10^7 cells/ml. The two populations were mixed at a 1:1 ratio and injected i.v. into recipient mice. Recipients were bled the next day, and PBMCs were analyzed for CFSE staining by flow cytometry.

Leukocyte preparations and purification of NK cells and CD8$^+$ T cells. Noninfected or infected mice were killed, and spleens were removed in RPMI, FCS 10%, minced, and filtered through 70-μm nylon mesh. RBCs were lysed with RBC lysis buffer (Sigma-Aldrich), and splenocytes were resuspended in complete medium. The enrichment of NK cells or CD8$^+$ T cells from splenocytes was performed using the NK cell isolation kit or the CD8$^+$ T cell isolation kit, respectively (Miltenyi Biotec). Cells of each type were counted, resuspended in RPMI, FCS 5%, and used in subsequent experiments.

In vitro assay for NK cell function and CD8$^+$ T cell function. To determine their cytolytic function, enriched NK cells were isolated from splenocytes 48 h after MCMV infection and incubated with YAC-1 cells at 37°C for 6 h. The percent-specific lysis was measured according to the release of lactate dehydrogenase into the supernatant, using the CytoTox 96 Non-Radioactive Cytotoxicity Assay (Promega). The degranulation capacity of NK cells was assayed by incubating NK cells with plate-bound antibodies directed against NK cell receptors (NK1.1, NKp46, and Ly49D, as indicated) for 4 h in the presence of FITC-conjugated anti–mouse CD107a (BD Biosciences) and monensin (Golgi-Stop; BD Biosciences). Enriched CD8$^+$ T cells were stimulated with PMA and ionomycin in the presence of brefeldin A (Golgi-Plug; BD Biosciences) for 4 h to measure IFN-γ synthesis, or with PMA and ionomycin in the presence of FITC-antiCD107a for 4 h to measure their degranulation. Splenocytes from LCMV-infected

mice were stimulated with the LCMV peptide GP33 or with the irrelevant HIV-derived peptide GP160 for 4 h in the presence of brefeldin A (GolgiPlug; BD Biosciences), after which IFN-γ production was measured by intracellular staining.

Antibodies, intracellular staining, and statistical analysis. Antibodies used in this study included the following: NK1.1 (PK136), IFN-γ (XMG1.2), CD8α (53-6.7), CD80 (B7-1), CD11b (M1/70), CD69 (H1.2F3; eBioscience), CD3ε (145-2C11), Ly49D (4E5), CD107a (1D4B; BD Biosciences), NKp46 (R&D Systems), F4/80 (BM8; Caltag laboratories). Intracellular staining was performed after classical staining for surface markers. Cells were then fixed and permeabilized using Cytofix/Cytoperm solution (BD Biosciences) for 20 min at 4°C, and then stained with IFN-γ antibody diluted in permeabilization buffer provided by BD Biosciences. All statistics were calculated using the Student's *t* test (two tail). *, $P < 0.05$; **, $P < 0.01$; ***, $P < 0.001$ in all figures. Error bars show SEM.

Online supplemental material. Table S1 shows a list and positions of the markers used for *Jinx* mapping using the C57BL/6 and C57BL/10 strains. Table SII shows a list and positions of markers identified in our laboratory and used for *Jinx* fine mapping on C57BL/6, C57BL/10, and C3H/HeN strains. In Fig. S1, mice (*Jinx* homozygotes and WT C57BL/6J controls) were infected with 2×10^4 PFU of MCMV and observed over a period of 14 d. Although the control animals did not appear ill at any time during the infection, the *Jinx* mice did show signs of sickness at day 5, with resolution by day 12. Mice were bled at days 7 and 14 for complete blood counts. Mice were killed at day 14 for visual inspection and weighing for the liver, spleen, and salivary glands. The online supplemental material is available at http://www.jem.org/cgi/content/full/jem.20062447/DC1.

The authors would like to thank Dr. Elina Zuniga and Prof. Michael B.A. Oldstone (TSRI) for providing cells, virus, and reagents, and for technical advice, as well as Dr. Thierry Walzer (CIML, Marseille, France) for helpful discussions.

This work was supported by National Institutes of Health grant number AI054523. S. Rutschmann was supported by a Human Frontier Science Program long-term fellowship. This is TSRI manuscript number 18610.

The authors have no conflicting financial interests.

Submitted: 21 November 2006
Accepted: 28 February 2007

REFERENCES

1. Arase, H., E.S. Mocarski, A.E. Campbell, A.B. Hill, and L.L. Lanier. 2002. Direct recognition of cytomegalovirus by activating and inhibitory NK cell receptors. *Science*. 296:1323–1326.
2. Lee, S.H., S. Girard, D. Macina, M. Busa, A. Zafer, A. Belouchi, P. Gros, and S.M. Vidal. 2001. Susceptibility to mouse cytomegalovirus is associated with deletion of an activating natural killer cell receptor of the C-type lectin superfamily. *Nat. Genet*. 28:42–45.
3. Lee, S.H., A. Zafer, Y. de Repentigny, R. Kothary, M.L. Tremblay, P. Gros, P. Duplay, J.R. Webb, and S.M. Vidal. 2003. Transgenic expression of the activating natural killer receptor Ly49H confers resistance to cytomegalovirus in genetically susceptible mice. *J. Exp. Med*. 197:515–526.
4. Brown, M.G., A.O. Dokun, J.W. Heusel, H.R. Smith, D.L. Beckman, E.A. Blattenberger, C.E. Dubbelde, L.R. Stone, A.A. Scalzo, and W.M. Yokoyama. 2001. Vital involvement of a natural killer cell activation receptor in resistance to viral infection. *Science*. 292:934–937.
5. Crozat, K., P. Georgel, S. Rutschmann, N. Mann, X. Du, K. Hoebe, and B. Beutler. 2006. Analysis of the MCMV resistome by ENU mutagenesis. *Mamm. Genome*. 17:398–406.
6. Beutler, B., K. Crozat, J.A. Koziol, and P. Georgel. 2005. Genetic dissection of innate immunity to infection: the mouse cytomegalovirus model. *Curr. Opin. Immunol*. 17:36–43.
7. Delale, T., A. Paquin, C. Asselin-Paturel, M. Dalod, G. Brizard, E.E. Bates, P. Kastner, S. Chan, S. Akira, A. Vicari, et al. 2005. MyD88-dependent and -independent murine cytomegalovirus sensing for IFN-alpha release and initiation of immune responses in vivo. *J. Immunol*. 175:6723–6732.
8. Krug, A., A.R. French, W. Barchet, J.A. Fischer, A. Dzionek, J.T. Pingel, M.M. Orihuela, S. Akira, W.M. Yokoyama, and M. Colonna. 2004. TLR9-dependent recognition of MCMV by IPC and DC generates coordinated cytokine responses that activate antiviral NK cell function. *Immunity*. 21:107–119.
9. Tabeta, K., P. Georgel, E. Janssen, X. Du, K. Hoebe, K. Crozat, S. Mudd, L. Shamel, S. Sovath, J. Goode, et al. 2004. Toll-like receptors 9 and 3 as essential components of innate immune defense against mouse cytomegalovirus infection. *Proc. Natl. Acad. Sci. USA*. 101:3516–3521.
10. Tabeta, K., K. Hoebe, E.M. Janssen, X. Du, P. Georgel, K. Crozat, S. Mudd, N. Mann, S. Sovath, J. Goode, et al. 2006. The Unc93b1 mutation 3d disrupts exogenous antigen presentation and signaling via Toll-like receptors 3, 7 and 9. *Nat. Immunol*. 7:156–164.
11. Hoebe, K., X. Du, P. Georgel, E. Janssen, K. Tabeta, S.O. Kim, J. Goode, P. Lin, N. Mann, S. Mudd, et al. 2003. Identification of Lps2 as a key transducer of MyD88-independent TIR signalling. *Nature*. 424:743–748.
12. Sjolin, H., E. Tomasello, M. Mousavi-Jazi, A. Bartolazzi, K. Karre, E. Vivier, and C. Cerboni. 2002. Pivotal role of KARAP/DAP12 adaptor molecule in the natural killer cell–mediated resistance to murine cytomegalovirus infection. *J. Exp. Med*. 195:825–834.
13. Presti, R.M., J.L. Pollock, A.J. Dal Canto, A.K. O'Guin, and H.W. Virgin IV. 1998. Interferon γ regulates acute and latent murine cytomegalovirus infection and chronic disease of the great vessels. *J. Exp. Med*. 188:577–588.
14. Pien, G.C., A.R. Satoskar, K. Takeda, S. Akira, and C.A. Biron. 2000. Cutting edge: selective IL-18 requirements for induction of compartmental IFN-gamma responses during viral infection. *J. Immunol*. 165:4787–4791.
15. Salazar-Mather, T.P., C.A. Lewis, and C.A. Biron. 2002. Type I interferons regulate inflammatory cell trafficking and macrophage inflammatory protein 1alpha delivery to the liver. *J. Clin. Invest*. 110:321–330.
16. Salazar-Mather, T.P., and K.L. Hokeness. 2003. Calling in the troops: regulation of inflammatory cell trafficking through innate cytokine/chemokine networks. *Viral Immunol*. 16:291–306.
17. Strobl, B., I. Bubic, U. Bruns, R. Steinborn, R. Lajko, T. Kolbe, M. Karaghiosoff, U. Kalinke, S. Jonjic, and M. Muller. 2005. Novel functions of tyrosine kinase 2 in the antiviral defense against murine cytomegalovirus. *J. Immunol*. 175:4000–4008.
18. Durbin, J.E., R. Hackenmiller, M.C. Simon, and D.E. Levy. 1996. Targeted disruption of the mouse Stat1 gene results in compromised innate immunity to viral disease. *Cell*. 84:443–450.
19. Lee, C.K., D.T. Rao, R. Gertner, R. Gimeno, A.B. Frey, and D.E. Levy. 2000. Distinct requirements for IFNs and STAT1 in NK cell function. *J. Immunol*. 165:3571–3577.
20. Nguyen, K.B., T.P. Salazar-Mather, M.Y. Dalod, J.B. Van Deusen, X.Q. Wei, F.Y. Liew, M.A. Caligiuri, J.E. Durbin, and C.A. Biron. 2002. Coordinated and distinct roles for IFN-alpha beta, IL-12, and IL-15 regulation of NK cell responses to viral infection. *J. Immunol*. 169:4279–4287.
21. Shellam, G.R., J.E. Allan, J.M. Papadimitriou, and G.J. Bancroft. 1981. Increased susceptibility to cytomegalovirus infection in beige mutant mice. *Proc. Natl. Acad. Sci. USA*. 78:5104–5108.
22. Loh, J., D.T. Chu, A.K. O'Guin, W.M. Yokoyama, and H.W. Virgin IV. 2005. Natural killer cells utilize both perforin and gamma interferon to regulate murine cytomegalovirus infection in the spleen and liver. *J. Virol*. 79:661–667.
23. Haddad, E.K., X. Wu, J.A. Hammer III, and P.A. Henkart. 2001. Defective granule exocytosis in Rab27a-deficient lymphocytes from Ashen mice. *J. Cell Biol*. 152:835–842.
24. Stinchcombe, J., G. Bossi, and G.M. Griffiths. 2004. Linking albinism and immunity: the secrets of secretory lysosomes. *Science*. 305:55–59.
25. Rubio, V., T.B. Stuge, N. Singh, M.R. Betts, J.S. Weber, M. Roederer, and P.P. Lee. 2003. Ex vivo identification, isolation and analysis of tumor-cytolytic T cells. *Nat. Med*. 9:1377–1382.

26. Alter, G., J.M. Malenfant, and M. Altfeld. 2004. CD107a as a functional marker for the identification of natural killer cell activity. *J. Immunol. Methods*. 294:15–22.
27. Feldmann, J., I. Callebaut, G. Raposo, S. Certain, D. Bacq, C. Dumont, N. Lambert, M. Ouachee-Chardin, G. Chedeville, H. Tamary, et al. 2003. Munc13-4 is essential for cytolytic granules fusion and is mutated in a form of familial hemophagocytic lymphohistiocytosis (FHL3). *Cell*. 115:461–473.
28. Marcenaro, S., F. Gallo, S. Martini, A. Santoro, G.M. Griffiths, M. Arico, L. Moretta, and D. Pende. 2006. Analysis of natural killer-cell function in familial hemophagocytic lymphohistiocytosis (FHL): defective CD107a surface expression heralds Munc13-4 defect and discriminates between genetic subtypes of the disease. *Blood*. 108:2316–2323.
29. Stepp, S.E., R. Dufourcq-Lagelouse, F. Le Deist, S. Bhawan, S. Certain, P.A. Mathew, J.I. Henter, M. Bennett, A. Fischer, G. de Saint Basile, and V. Kumar. 1999. Perforin gene defects in familial hemophagocytic lymphohistiocytosis. *Science*. 286:1957–1959.
30. zur Stadt, U., S. Schmidt, B. Kasper, K. Beutel, A.S. Diler, J.I. Henter, H. Kabisch, R. Schneppenheim, P. Nurnberg, G. Janka, and H.C. Hennies. 2005. Linkage of familial hemophagocytic lymphohistiocytosis (FHL) type-4 to chromosome 6q24 and identification of mutations in syntaxin 11. *Hum. Mol. Genet*. 14:827–834.
31. Menasche, G., E. Pastural, J. Feldmann, S. Certain, F. Ersoy, S. Dupuis, N. Wulffraat, D. Bianchi, A. Fischer, F. Le Deist, and G. de Saint Basile. 2000. Mutations in RAB27A cause Griscelli syndrome associated with haemophagocytic syndrome. *Nat. Genet*. 25:173–176.
32. Rubin, C.M., B.A. Burke, R.W. McKenna, K.L. McClain, J.G. White, M.E. Nesbit Jr., and A.H. Filipovich. 1985. The accelerated phase of Chediak-Higashi syndrome. An expression of the virus-associated hemophagocytic syndrome? *Cancer*. 56:524–530.
33. Fisman, D.N. 2000. Hemophagocytic syndromes and infection. *Emerg. Infect. Dis*. 6:601–608.
34. Badovinac, V.P., A.R. Tvinnereim, and J.T. Harty. 2000. Regulation of antigen-specific CD8+ T cell homeostasis by perforin and interferon-gamma. *Science*. 290:1354–1358.
35. Matloubian, M., M. Suresh, A. Glass, M. Galvan, K. Chow, J.K. Whitmire, C.M. Walsh, W.R. Clark, and R. Ahmed. 1999. A role for perforin in downregulating T-cell responses during chronic viral infection. *J. Virol*. 73:2527–2536.
36. Kagi, D., B. Odermatt, and T.W. Mak. 1999. Homeostatic regulation of CD8+ T cells by perforin. *Eur. J. Immunol*. 29:3262–3272.
37. Jordan, M.B., D. Hildeman, J. Kappler, and P. Marrack. 2004. An animal model of hemophagocytic lymphohistiocytosis (HLH): CD8+ T cells and interferon gamma are essential for the disorder. *Blood*. 104:735–743.
38. Henter, J.I., G. Elinder, and A. Ost. 1991. Diagnostic guidelines for hemophagocytic lymphohistiocytosis. The FHL Study Group of the Histiocyte Society. *Semin. Oncol*. 18:29–33.
39. Henter, J.I., A. Horne, M. Arico, R.M. Egeler, A.H. Filipovich, S. Imashuku, S. Ladisch, K. McClain, D. Webb, J. Winiarski, and G. Janka. 2007. HLH-2004: diagnostic and therapeutic guidelines for hemophagocytic lymphohistiocytosis. *Pediatr. Blood Cancer*. 48:124–131.
40. Madison, J.M., S. Nurrish, and J.M. Kaplan. 2005. UNC-13 interaction with syntaxin is required for synaptic transmission. *Curr. Biol*. 15:2236–2242.
41. Brose, N., K. Hofmann, Y. Hata, and T.C. Sudhof. 1995. Mammalian homologues of Caenorhabditis elegans unc-13 gene define novel family of C2-domain proteins. *J. Biol. Chem*. 270:25273–25280.
42. Ahmed, S., I.N. Maruyama, R. Kozma, J. Lee, S. Brenner, and L. Lim. 1992. The Caenorhabditis elegans unc-13 gene product is a phospholipid-dependent high-affinity phorbol ester receptor. *Biochem. J*. 287:995–999.
43. Augustin, I., C. Rosenmund, T.C. Sudhof, and N. Brose. 1999. Munc13-1 is essential for fusion competence of glutamatergic synaptic vesicles. *Nature*. 400:457–461.
44. Varoqueaux, F., A. Sigler, J.S. Rhee, N. Brose, C. Enk, K. Reim, and C. Rosenmund. 2002. Total arrest of spontaneous and evoked synaptic transmission but normal synaptogenesis in the absence of Munc13-mediated vesicle priming. *Proc. Natl. Acad. Sci. USA*. 99:9037–9042.
45. Augustin, I., S. Korte, M. Rickmann, H.A. Kretzschmar, T.C. Sudhof, J.W. Herms, and N. Brose. 2001. The cerebellum-specific Munc13 isoform Munc13-3 regulates cerebellar synaptic transmission and motor learning in mice. *J. Neurosci*. 21:10–17.
46. Varoqueaux, F., M.S. Sons, J.J. Plomp, and N. Brose. 2005. Aberrant morphology and residual transmitter release at the Munc13-deficient mouse neuromuscular synapse. *Mol. Cell. Biol*. 25:5973–5984.
47. Verhage, M., A.S. Maia, J.J. Plomp, A.B. Brussaard, J.H. Heeroma, H. Vermeer, R.F. Toonen, R.E. Hammer, T.K. van den Berg, M. Missler, et al. 2000. Synaptic assembly of the brain in the absence of neurotransmitter secretion. *Science*. 287:864–869.
48. Shirakawa, R., T. Higashi, A. Tabuchi, A. Yoshioka, H. Nishioka, M. Fukuda, T. Kita, and H. Horiuchi. 2004. Munc13-4 is a GTP-Rab27-binding protein regulating dense core granule secretion in platelets. *J. Biol. Chem*. 279:10730–10737.
49. Bossi, G., and G.M. Griffiths. 1999. Degranulation plays an essential part in regulating cell surface expression of Fas ligand in T cells and natural killer cells. *Nat. Med*. 5:90–96.
50. Blott, E.J., and G.M. Griffiths. 2002. Secretory lysosomes. *Nat. Rev. Mol. Cell Biol*. 3:122–131.
51. Du, X., K. Tabeta, K. Hoebe, H. Liu, N. Mann, S. Mudd, K. Crozat, S. Sovath, X. Gong, and B. Beutler. 2004. Velvet, a dominant Egfr mutation that causes wavy hair and defective eyelid development in mice. *Genetics*. 166:331–340.
52. Orange, J.S., B. Wang, C. Terhorst, and C.A. Biron. 1995. Requirement for natural killer cell–produced interferon γ in defense against murine cytomegalovirus infection and enhancement of this defense pathway by interleukin 12 administration. *J. Exp. Med*. 182:1045–1056.
53. Dutko, F.J., and M.B. Oldstone. 1983. Genomic and biological variation among commonly used lymphocytic choriomeningitis virus strains. *J. Gen. Virol*. 64:1689–1698.